Hindawi
Advances in Materials Science and Engineering
Volume 2022, Article ID 9150442, 11 pages
https://doi.org/10.1155/2022/9150442

Research Article

Synthesis and Characterization of Mechanical Properties of AA8014 + Si_3N_4/ ZrO_2 Hybrid Composites by Stir Casting Process

C. Ramesh Kannan,[1] R. Venkatesh,[2] M. Vivekanandan,[3] J. Phani Krishna,[4] S. Manivannan,[5] S. Rajkumar ,[6] and V. Vijayan [7]

[1]*Department of Mechanical Engineering, Dr.Navalar Nedunchezhiyan College of Engineering, Tholudur, India*
[2]*Department of Mechanical Engineering, Saveetha School of Engineering, SIMATS, Chennai 602105, Tamilnadu, India*
[3]*Department of Mechanical Engineering, National Engineering College, Kovilpatti-628503, Tamilnadu, India*
[4]*Powder Handling Solutions, RIECO Industries Ltd, Pune 411 005, India*
[5]*Centre for Material Science, Department of Mechanical Engineering, Karpagam Academy of Higher Education, Coimbatore 641021, India*
[6]*Department of Mechanical Engineering, Faculty of Manufacturing, Institute of Technology, Hawassa University, Hawassa, Ethiopia*
[7]*Department of Mechanical Engineering, K.Ramakrishnan College of Technology, Samayapuram Trichy 621 112, Tamil Nadu, India*

Correspondence should be addressed to S. Rajkumar; rajkumar@hu.edu.et

Received 26 October 2021; Revised 17 December 2021; Accepted 20 December 2021; Published 4 January 2022

Academic Editor: Fuat Kara

Lightweight materials are extremely needed for the manufacturing of industrial parts and are used in aerospace, automobile body shops, biomedical instruments, etc. Aluminium alloy is one of the light-weight materials, and it fulfills the industrial demands based on their natural strength/stiffness, enhanced temperature permanence, superior wear, and corrosion resistance. This experimental work considered aluminium alloy (AA8014) with reinforced particles of silicon nitride (Si_3N_4) and zirconium dioxide (ZrO_2) for preparing aluminium hybrid composites. Hybrid composites are prepared by a stir casting process involving different process parameters. L27 orthogonal array is used for optimizing the stir casting parameters with the assistance of the statistical Taguchi approach. Stir casting parameters are the percentage of reinforcement (4%, 6%, and 8%), stir speed (400 rpm, 500 rpm, and 600 rpm), stir time (20 min, 25 min, and 30 min), and molten temperature (700 °C, 800 °C, and 900 °C). Mechanical performance such as wear and microhardness of the hybrid composites is evaluated. Minimum wear and higher microhardness are encountered at a percentage of reinforcement = 6%, stir speed = 400 rpm, stir time = 30 min, and molten temperature = 900°C. In wear analysis, the percentage of reinforcement highly influences the wear properties (7.06% contribution). In microhardness analysis, molten temperature parameter is the extreme influencer (11.15% contribution).

1. Introduction

Recently, the aircraft, marine, and automobile sectors need more light-weight materials for the construction of structural work and manufacturing of components [1]. Hybrid composites are generally built for improving the performance of the material in specific applications and their easy processability during manufacturing of the component for application. These hybrid composites have gained a lot of interest in recent times due to their excellent functionality for prescribed applications. Loads of studies have been carried out by the researchers using different combinations of reinforcement materials. Most of the researchers concentrate on a combination of metal-ceramic reinforcement and metal-fiber reinforcement [2]. Based on utilization, the material properties can be changed through the reinforcement of hard particles to the lightweight materials. Reinforced particles onto the alloy material are termed as

"composites," and two or more reinforced particles occupied in the base alloy are termed as "hybrid composites" [3]. Composites based on AA7075, Si_3N_4, and MoS_2 recorded an increased density when the MoS_2 proportion increased. A decrease of 16% in microhardness, 36% in compressive strength, and 37% in COF was recorded with increase in MoS_2 proportion [4]. An investigation at the elevated tribological behaviour of Al/SiC/MoS_2 composite cased with AA5059 alloy, 2% MoS_2, and varying percentage of SiC reinforcement revealed that the wear and COF of the casted component reduced with increase in SiC reinforcement. Also, the investigation revealed that the temperature has a significant impact on the friction and wear behaviour of cast composites [5]. In a study conducted, the function of MoS_2 as a solid lubricant in different base matrices such as aluminium, copper, iron, and silver was outlined. The researchers compiled and displayed a comprehensive review of different testing setups, the influence of environmental circumstances, and the operational parameters on the wear and friction of MoS_2-added composites [6]. Low specific gravity properties improved the modulus and strength of the composite materials when compared to other engineering materials. In metal matrix composites, the pure metal or alloys are the matrix materials, and the hard particles are reinforced particles [7]. When the proportion of Si_3N_4 particles was increased, the microhardness of the composite material raised by 25%, which could be attributed to a rise in the hard ceramic phase. The compressive strength of concrete increased significantly by 1.1 times when the proportion of Si_3N_4 particles was increased, which may be attributed to the hard ceramic reinforcement's workability at elevated loads. Normally, aluminium and its alloys are widely used in metal matrix composites due to their superior properties, namely, low electrical resistance, elevated strength, and excellent corrosion resistance [8]. The addition of reinforced particles enhanced the wear properties of the aluminium alloys. The stir casting process is highly involved in the preparation of composites [9]. Different stir casting parameters, namely, stirring speed, stirring time, and molten temperature, are utilized for the fabrication of effective composites. Stirring action can be controlled by coupled electric motor in the stirring unit; it enhances the stirring action and offers an excellent blending of composite materials [10]. This study was effectively conducted through a dry sliding wear test apparatus employed with effective parameters. More number of wear test investigations are conducted in the aluminium metal matrix composites [11]. SiC reinforced composites also outperformed the matrix alloy in terms of wear resistance. In the case of matrix alloys, the wear mechanism was pliable; however, in the scenario of SiC reinforced composites, the wear mechanism changed to be abrasive [12]. The two main parameters influencing AMCs are the size of the reinforcement and its fraction volume. The combination of a high reinforcement volume concentration and lower particle size is added to the strength development of AMCs [13]. Reinforced particles are enhanced by the wear performance of the composite materials. Microhardness is one of the mechanical properties to assess the hardness of the material through the Vickers hardness tester [14]. Some of the components need more hardness; hence, hardness can be improved by the reinforcement of hard particles through the powder metallurgy route or the stir casting process. In the stir casting process, the reinforced particles are blended homogeneously and extremely increase the hardness of the material [15]. In a study, stir casting was used to create an Al6061 composite reinforced with varying amounts of TiB_2 particles. Optimizing the parameters resulted in a homogenous distribution of reinforcements (TiB_2) in the aluminium matrix with no aggregation, and sturdy bonding was witnessed with K_2TiF_6 inclusion and preheating of TiB_2 powders before incorporating to the melting point. The tensile strength of composite samples was increased without a substantial reduction in elongation to failure by increasing the mass of TiB_2 reinforcing particles [16]. The density and hardness of an Al-based matrix composite enhanced with SiC increase linearly with weight fraction. Wear properties improved significantly in the presence of SiC particles. The addition of 5% SiCp to an arbitrarily aged Al2024 alloy and SiC-based composite increased the fatigue resistance up to 100%. Furthermore, the integration of SiCp simplifies the structure while also increasing the modulus and strength during yielding [17]. The aim of this experimental work was to prepare aluminium hybrid composites such as using aluminium alloy (AA8014) with reinforced particles (silicon nitride and zirconium dioxide) through the stir casting process.Taguchi approach was used to optimize the stir casting parameters and improved the wear and microhardness of the hybrid composites [18].

From the above literature review, it is seen that very limited work has been carried out with the below-mentioned parameter levels and the combination of the materials selected. The primary motto of this research is to analyze the impact of the reinforcements and the selected parameters on the variation in the mechanical and tribological properties of the composites under investigation. The parts are casted out using a stir casting machine, and the wear behavior is analyzed with the help of the pin on disc wear testing machine. Also, microhardness is measured using the Vickers hardness testing machine. Taguchi's optimization technique is used to identify the commendable parameter combinations for the selected responses.

2. Materials and Methods

In this experimental work, aluminium alloy AA8014 is used as the base material, and the reinforced particles are silicon nitride and zirconium dioxide. All these materials are procured in Nualco Private Limited, Ambattur Industrial Estate, Chennai, for the required quantity. All the constituent elements are present in AA8014, as presented in Table 1.

The stir casting method is implemented for this experimental work for effective composite preparation to conduct wear and microhardness analysis [19–21].

Classically, the responses are grouped into three major wings. Signal-to-noise ratio is predominately applied to identify the degree of peripheral instabilities that occur within the system *t* and improve the efficacy and accuracy of

Table 1: Chemical composition of AA8014.

Element	Content (%)
Iron	1.4
Silicon	0.28
Manganese	0.40
Copper	0.18
Zinc	0.008
Titanium	0.008
Magnesium (Mg)	0.10
Aluminium	Balance

experimentation [22]. The three conditions and the formulae to find the S/N ratio is given in equations (1)–(3).

Lesser the better (wear rate):

$$\frac{S}{N} = -10 \log\left(\frac{1}{a}\sum_{i=1}^{a} z_i^2\right). \quad (1)$$

Higher the better (microhardness):

$$\frac{S}{N} = -10 \log\left(\frac{1}{a}\sum_{i=1}^{a} \frac{1}{z_i^2}\right). \quad (2)$$

Nominal the best (dimensional tolerance):

$$\frac{S}{N} = -10 \log\left(\frac{1}{a}\sum_{i=1}^{a} \frac{z'}{V_z^2}\right), \quad (3)$$

where Z' represents the i^{th} experiment's value, and a is the number of replications of each test.

3. Experimental Procedure

The stir casting process is considered for this investigation to make a hybrid composite. The schematic view of the stir casting process is illustrated in Figure 1. The preheating process of the reinforced particles (silicon nitride and zirconium oxide) is conducted in the crucible with the different weight percentages (4%, 6%, and 8%). This process was maintained at 550 °C for 4 hours in the crucible for removing impurities present in the reinforced particles [22–24]. The preheating process removes the impurities present in the reinforced particles. The base aluminium alloy is heated with 900 °C using a bottom pouring furnace; continually, both the heated materials are mixed well with the help of a stirring action [25]. Since the number of parameters under consideration is four and their respective levels are 3, the number of experimentations required for analysis is determined to be 27 based on Taguchi's orthogonal array method (L27).

Applying different weight percentages of reinforced particles, stir speed, stir time, and molten temperature, the stir casting process is effectively carried out [26]. Finally, the molten material is poured into the prepared die to obtain the required samples. Based on the wear test and microhardness test, the specimens are cut out from the casted hybrid composites [27].

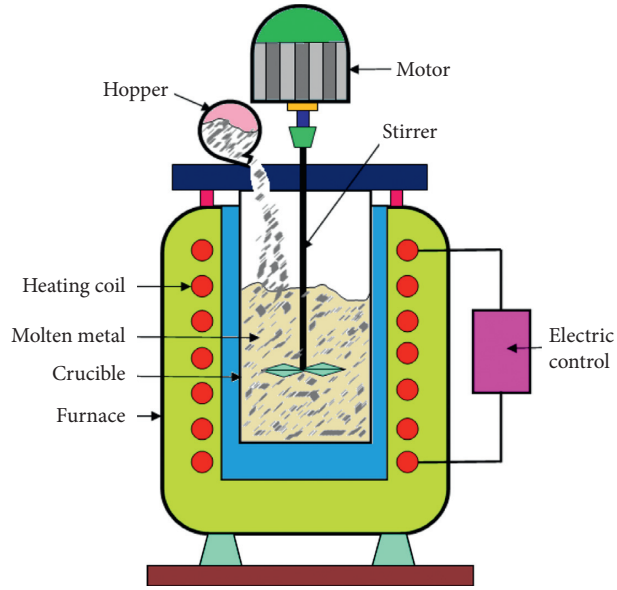

Figure 1: Schematic view of stir casting process.

3.1. Wear Test. Using the DUCOM model dry sliding wear test apparatus, the wear test is carried out effectively, and the wear test specimens are prepared under the ASTM G99 standard [28]. The specimen's dimensions are 12 mm diameter and 35 mm length, as shown in Figure 2(b). Before conducting the wear test, the rotating disc and all specimens are cleaned well using acetone, and all the specimens are initially weighed for calculating mass loss or wear loss in the final stage [29]. Specimens are positioned vertically and touch the rotating disc. The wear parameters are chosen as load 35 N, disc speed 3 m/s, sliding distance 1500 m, and time period 30 min. After conducting the wear test, the weight of each sample is measured using the digital weight balance. Both initial weight and final weight of the samples are used to calculate the wear, wear rate, friction, etc.

3.2. Microhardness Test. ASTM E384 is the standard test method for conducting the microhardness test on the materials [30]. The indentation is created in the test specimen using an intender made with diamond under a very smaller loading condition. The typical variation in load that can be done in a Vickers hardness testing machine is from 0.01 kgf to 1 kgf (0.098 N to 9.81 N). The microhardness test is conducted through the Vickers hardness testing machine under a load of 0.5 kgf (4.90 N). All the samples are cleaned thoroughly; each specimen is tested more than three times; finally, it is averaged.

Table 2 illustrates different stir casting parameters and their levels. Different stir casting parameters are % of reinforcement, stir speed (rpm), stir time (min), and molten temperature (°C).

4. Results and Discussion

Table 3 presents the minimum wear and maximum hardness of all the samples with the influence of different

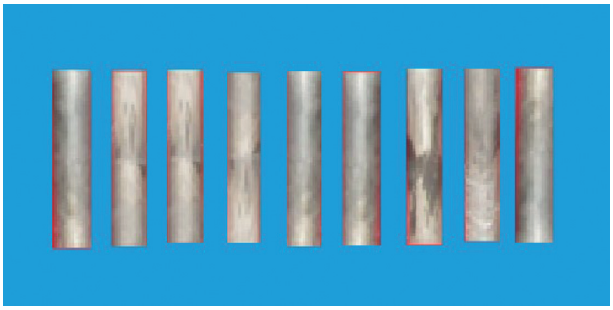

Figure 2: Wear test specimen image.

Table 2: Wear test process parameters and their levels.

S. No	Parameter	Level 1	Level 2	Level 3
1.	% of reinforcement	4	6	8
2.	Stir speed (rpm)	400	500	600
3.	Stir time (min)	20	25	30
4.	Molten temperature (°C)	700	800	900

Table 3: Experimental summary of wear and microhardness tests.

Exp. No.	% of reinforcement	Stir speed (rpm)	Stir time (min)	Molten temperature (°C)	Wear (mm^3/m)	Microhardness (VHN)	S/N ratio of wear	S/N ratio of microhardness
1	4	400	20	700	0.256	118	11.2687	41.4582
2	4	400	20	700	0.382	116	11.2687	41.4582
3	4	400	20	700	0.112	121	11.2687	41.4582
4	4	500	25	800	0.654	115	6.9550	41.0758
5	4	500	25	800	0.256	99	6.9550	41.0758
6	4	500	25	800	0.334	133	6.9550	41.0758
7	4	600	30	900	0.095	148	13.1822	42.6045
8	4	600	30	900	0.127	120	13.1822	42.6045
9	4	600	30	900	0.345	142	13.1822	42.6045
10	6	400	25	900	0.115	166	11.8289	42.5405
11	6	400	25	900	0.412	133	11.8289	42.5405
12	6	400	25	900	0.118	116	11.8289	42.5405
13	6	500	30	700	0.234	152	12.0737	41.3380
14	6	500	30	700	0.345	98	12.0737	41.3380
15	6	500	30	700	0.111	117	12.0737	41.3380
16	6	600	20	800	0.410	137	8.4767	41.8277
17	6	600	20	800	0.318	117	8.4767	41.8277
18	6	600	20	800	0.396	119	8.4767	41.8277
19	8	400	30	800	0.124	121	14.6033	43.0553
20	8	400	30	800	0.098	160	14.6033	43.0553
21	8	400	30	800	0.281	156	14.6033	43.0553
22	8	500	20	900	0.108	134	13.1902	41.8388
23	8	500	20	900	0.345	128	13.1902	41.8388
24	8	500	20	900	0.115	112	13.1902	41.8388
25	8	600	25	700	0.312	135	12.1783	40.8975
26	8	600	25	700	0.099	95	12.1783	40.8975
27	8	600	25	700	0.273	113	12.1783	40.8975

combinations of parameters. In this analysis, the minimum wear was recorded as 0.095 mm^3/m by influencing 4% of reinforcement, 600 rpm of stir speed, 30 min of stir time, and 900°C of molten temperature. From the microhardness analysis, the maximum hardness was obtained as 166 VHN by 6% of reinforcement, 400 rpm of stir speed, 25 min of stir time, and 900°C of molten temperature.

4.1. Wear Analysis. The percentage of reinforcement was highly influenced in the wear analysis, as presented in Tables 4 and 5. Based on the delta and rank order, the parameter influences were concluded. Stir time was the second priority, stir speed was the third priority, and molten temperature was the fourth priority. Optimal parameters were found as 8% of reinforcement, 400 rpm of stir speed, 30 min of stir time, and 900°C of molten temperature.

Table 4: Response table for means (wear test).

Level	% of reinforcement	Stir speed (rpm)	Stir time (min)	Molten temperature (°C)
1	0.2846	0.2109	0.2713	0.2360
2	0.2732	0.2780	0.2859	0.3190
3	0.1950	0.2639	0.1956	0.1978
Delta	0.1212	0.0896	0.0903	0.0671
Rank	1	3	2	4

Table 5: Response table for signal-to-noise ratios. Smaller is better.

Level	% of reinforcement	Stir speed (rpm)	Stir time (min)	Molten temperature (°C)
1	10.47	12.57	10.98	11.84
2	10.79	10.74	10.32	10.01
3	13.32	11.28	13.29	12.73
Delta	2.97	2.72	2.86	1.83
Rank	1	3	2	4

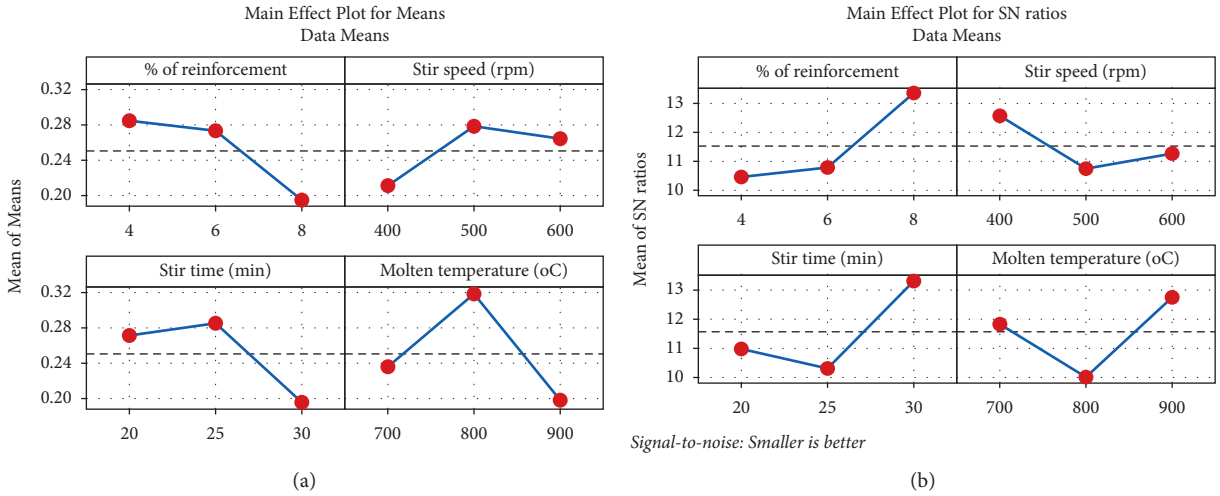

Figure 3: Main effects plots for wear test. (a) Means. (b) S/N ratio.

Increasing reinforcement percentage reduces the wear, and 8% of reinforcement offers minimum wear, as shown in Figure 3. The wear rate of the test specimens has decreased with the increase in % of reinforcement from 4% to 6% by 4.17%. Furthermore, when % of reinforcement is increased from 6% to 8%, the wear rate has again decreased by 40.10%. An overall decrease of 45% is seen with the increase of reinforcement. When the stir speed is increased from 400 rpm to 500 rpm, the wear rate has increased up to 24.14%, and an increase in stir speed beyond 500 rpm decreases the wear rate by 5.14%. The wear rate has increased by 5.14% when the stir time is increased from 20 min to 25 min. But, a drop of 46.17% is seen when the stir time is further increased from 25 min to 30 min. Minimum stir speed (400 rpm) recorded minimum wear of the hybrid composites. When the molten temperature is raised from 700 to 800 degrees, the wear rate increases by 26.02%. However, when the molten temperature is raised from 800 to 900 degrees, the drop is 61.27%. The hybrid composites wore out the least when stirred at the slowest possible speed (400 rpm). Minimum stir time increases the wear; further increases of stir time from 20 min to 30 min can raise the wear to a high level. Higher molten temperature 900 ° C recorded minimum wear compared to other temperature levels.

Normal probability plot, versus fits plot, histogram plot, and versus order plot were shown in the single graph such as residual plots, as it is shown in Figure 4. All these plots represented the selected parameters, and the data are the appropriate one for wear analysis.

Table 6 represents the analysis of variance for the wear test. This ANOVA analysis presented the contribution of each parameter from a lower to a higher order. Among the four parameters, the percentage of reinforcement was highly influenced such as it was contributed as 7.06%, followed by stir time (5.05%), stir speed (2.47%), and molten temperature (1.29%). Higher F-value denoted the higher contribution percentage level of the parameters.

Figure 5 illustrates the contour plot for the wear test; Figure 5(a) correlates the two parameters such as % of reinforcement and stir speed. From this correlation, minimum wear was recorded by the influence of maximum % of

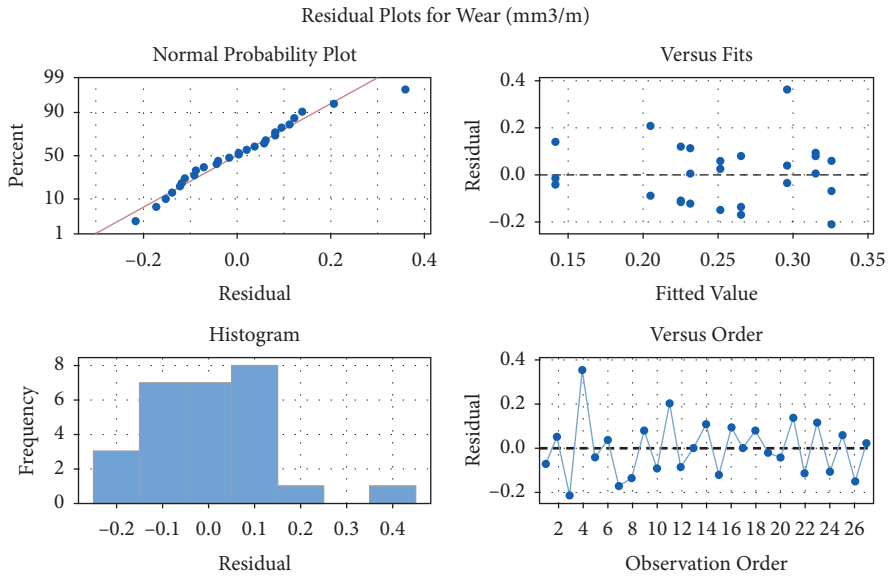

Figure 4: Residual plots for wear test.

Table 6: Analysis of variance for wear test.

Source	Df	Seq SS	Contribution (%)	Adj SS	Adj MS	F-value	*P*-value
Regression	4	0.081146	15.86	0.081146	0.020286	1.04	0.411
% of reinforcement	1	0.036091	7.06	0.036091	0.036091	1.84	0.188
Stir speed (rpm)	1	0.012641	2.47	0.012641	0.012641	0.65	0.430
Stir time (min)	1	0.025840	5.05	0.025840	0.025840	1.32	0.263
Molten temperature (°C)	1	0.006574	1.29	0.006574	0.006574	0.34	0.568

Wear (mm3/m) = 0.595 – 0.0224% of reinforcement + 0.000265 stir speed (rpm) – 0.00758 stir time (min) – 0.000191 molten temperature (°C).

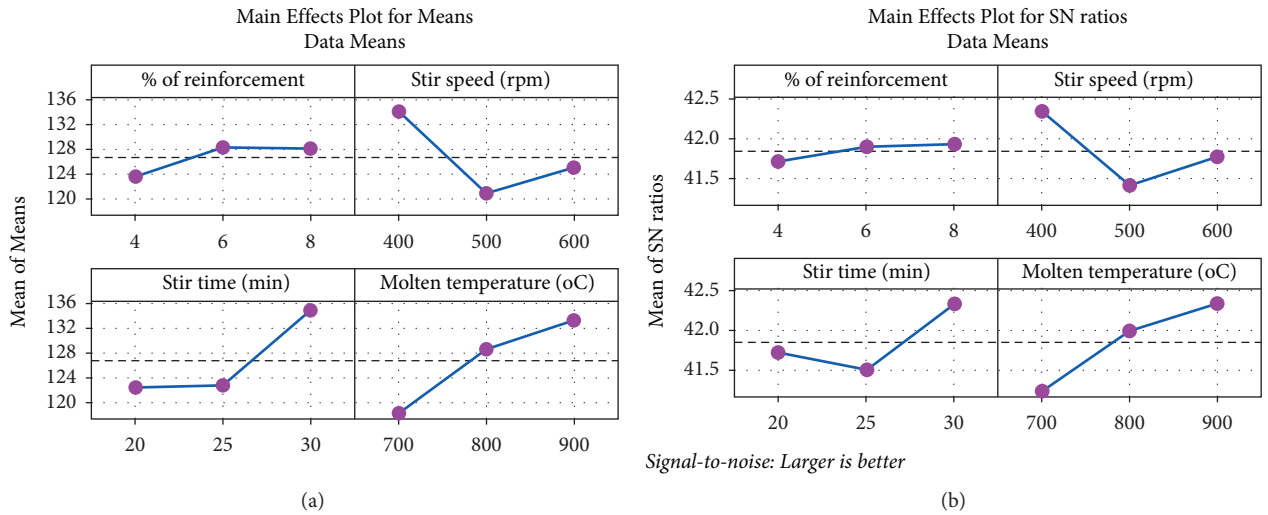

Figure 5: Contour plot for wear test: (a) % of reinforcement Vs stir speed, (b) stir speed Vs stir time, (c) stir time Vs molten temperature, and (d) molten temperature Vs % of reinforcement.

reinforcement and minimum level of stir speed. Minimum wear was recorded at 8% of reinforcement and 400 rpm of stir speed. The wear tends to increase in a linear mode when the stir speed is increased from 400 rpm to 600 rpm, whereas the wear decreases with an increase in % of reinforcement from 4% to 8%. Figure 5(b) illustrates the relations between stir speeds and stir time; both parameter relations of the minimum wear were recorded by the influence of the minimum stir speed and the maximum stir time. The minimum wear was recorded at 400 rpm of stir speed and 30 min of stir time. The wear tends to increase in a linear mode when the stir speed is increased from 400 rpm to

Table 7: Response table for means (microhardness).

Level	% of reinforcement	Stir speed (rpm)	Stir time (min)	Molten temperature (°C)
1	123.6	134.1	122.4	118.3
2	128.3	120.9	122.8	128.6
3	128.2	125.1	134.9	133.2
Delta	4.8	13.2	12.4	14.9
Rank	4	3	2	1

Table 8: Response table for signal-to-noise ratios (microhardness). Larger is better.

Level	% of reinforcement	Stir speed (rpm)	Stir time (min)	Molten temperature (°C)
1	41.71	42.35	41.71	41.23
2	41.90	41.42	41.50	41.99
3	41.93	41.78	42.33	42.33
Delta	0.22	0.93	0.83	1.10
Rank	4	3	2	1

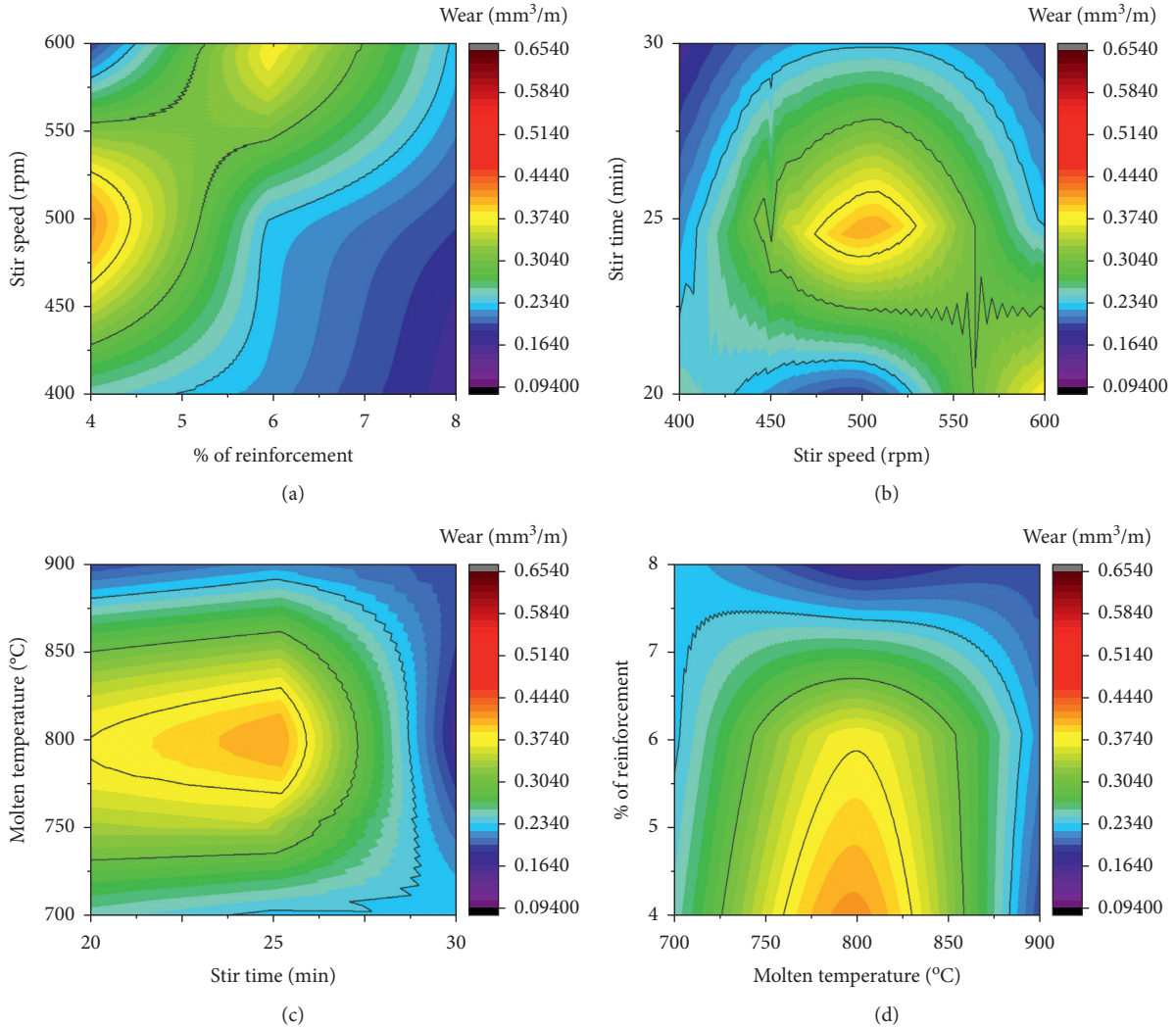

Figure 6: Main effect plot for microhardness test. (a) Means. (b) S/N ratio.

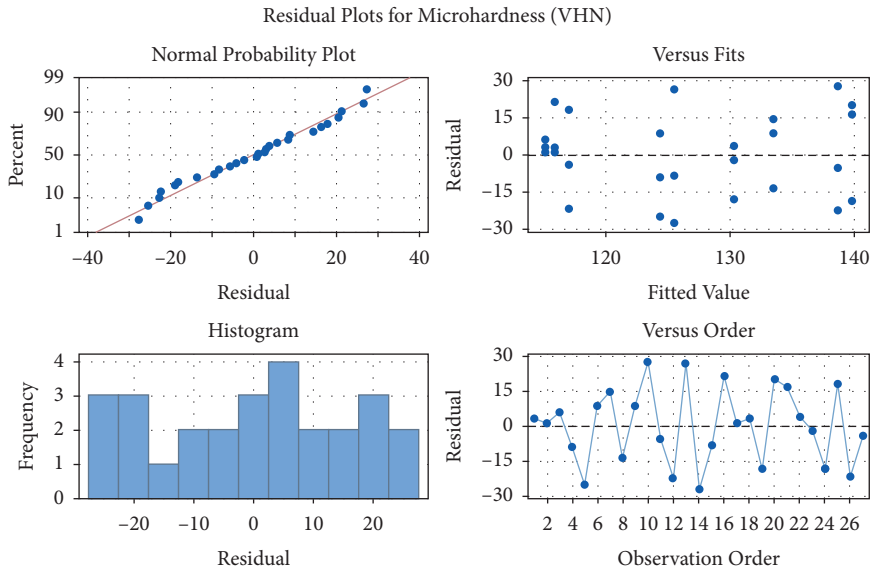

Figure 7: Residual plots for microhardness analysis.

600 rpm, whereas the wear decreases with an increase in stir time from 20 min to 30 min. Figure 5(c) represents the association between stir time and molten temperature. For this combination, the minimum wear was recorded by the influence of both parameters' values at a high level. The minimum wear was recorded at 30 min of stir time and 900 ^{0}C of molten temperature. The wear tends to decrease in a linear mode when molten temperature increases gradually and also decreases with an increase in stir time from 20 min to 30 min. Figure 5(d) illustrates the combination of molten temperature and % of reinforcement. For this combination, both the parameters' levels are higher and were offered minimum wear. Minimum wear was recorded at 900 ^{0}C of molten temperature and 8% of reinforcement. The wear tends to decrease in a linear mode when molten temperature increases gradually and also the wear increases with increase in % of reinforcement from 4% to 8%.

4.2. Microhardness Analysis. In the microhardness analysis, the molten temperature was extremely influenced, Tables 7 and 8. Furthermore, other parameter influences were decided by delta and rank order. The stir time was the second precedence parameter, stir speed was the third precedence, and % of reinforcement was the fourth precedence. In the microhardness analysis, the optimum parameters were recorded as 8% of reinforcement, 400 rpm of stir speed, 30 min of stir time, and 900 ^{o} C of molten temperature.

Minimum percentage of reinforcement such as 4% offered minimum hardness value; further increasing of reinforcement from 4% to 8% offered higher hardness values, as shown in Figure 6. The microhardness of the test specimens has raised with the increase in % of reinforcement from 4% to 6% by 3.66%. Furthermore, increase in % of reinforcement from 6 % to 8 % has no impact on the microhardness. When the stir speed is increased from 400 rpm to 500 rpm, the microhardness has decreased up to 10.92%, and an increase in the stir speed beyond 500 rpm increases the microhardness by 3.36%. Microhardness has increased by 0.33% when the stir time is increased from 20 min to 25 min (i.e., not much improvement is seen with an increase in the stir time). But a rise of 8.97% is seen when the stir time is further increased from 25 min to 30 min. When the molten temperature is raised from 700 to 800 degrees, the microhardness increases by 8.01%. However, when the molten temperature is raised from 800 to 900 degrees, the raise is 3.25%. The minimum stir speed of 400 rpm offered the maximum level of microhardness values. Continually increasing stir speed reduces the microhardness. The lower level of stir time reduces the hardness values; further increasing of stir time offered maximum hardness values. Initial 700 C molten temperature which offered minimum hardness values continually increases the molten temperature from 700^{o}C to 900^{o}C which recorded maximum hardness values.

All the four graphs in Figure 7 are presented in the single plot, namely, residual plot. It denotes that the selected model and the data values are accurate or not based on the scattered data points. Most of the data points are touches and are very close to the mean line in the probability plot. Both in the versus fits and versus order plots, the data points distributed constantly and all these represent the chosen model was a precise one. In the ANOVA analysis, higher contribution percentage of the parameters in the microhardness was evaluated. Higher contribution was recorded by the molten temperature such as 11.15% followed by stir time (7.79%), stir speed (4.07%), and percentage of reinforcement (1.10%), Table 9.

Figure 8 represents the 3D Trajectory plot for the microhardness test. Figure 8(a) illustrates the maximum hardness that was attained by the influence of 4% of reinforcement and 400 rpm of stir speed. Figure 8(b) illustrates the maximum microhardness values by the influence of 400 rpm of stir speed and 25 min of stir time. Figure 8(c)

Table 9: Analysis of Variance for microhardness test.

Source	Df	Seq SS	Contribution (%)	Adj SS	Adj MS	F-value	*P*-value
Regression	4	2156.94	24.11	2156.94	539.24	1.75	0.176
% of reinforcement	1	98.00	1.10	98.00	98.00	0.32	0.579
Stir speed (rpm)	1	364.50	4.07	364.50	364.50	1.18	0.289
Stir time (min)	1	696.89	7.79	696.89	696.89	2.26	0.147
Molten temperature (°C)	1	997.56	11.15	997.56	997.56	3.23	0.086

Microhardness (VHN) = 51.5 + 1.17% of reinforcement − 0.0450 Stir speed (rpm) + 1.244 Stir time (min) + 0.0744 Molten temperature (°C).

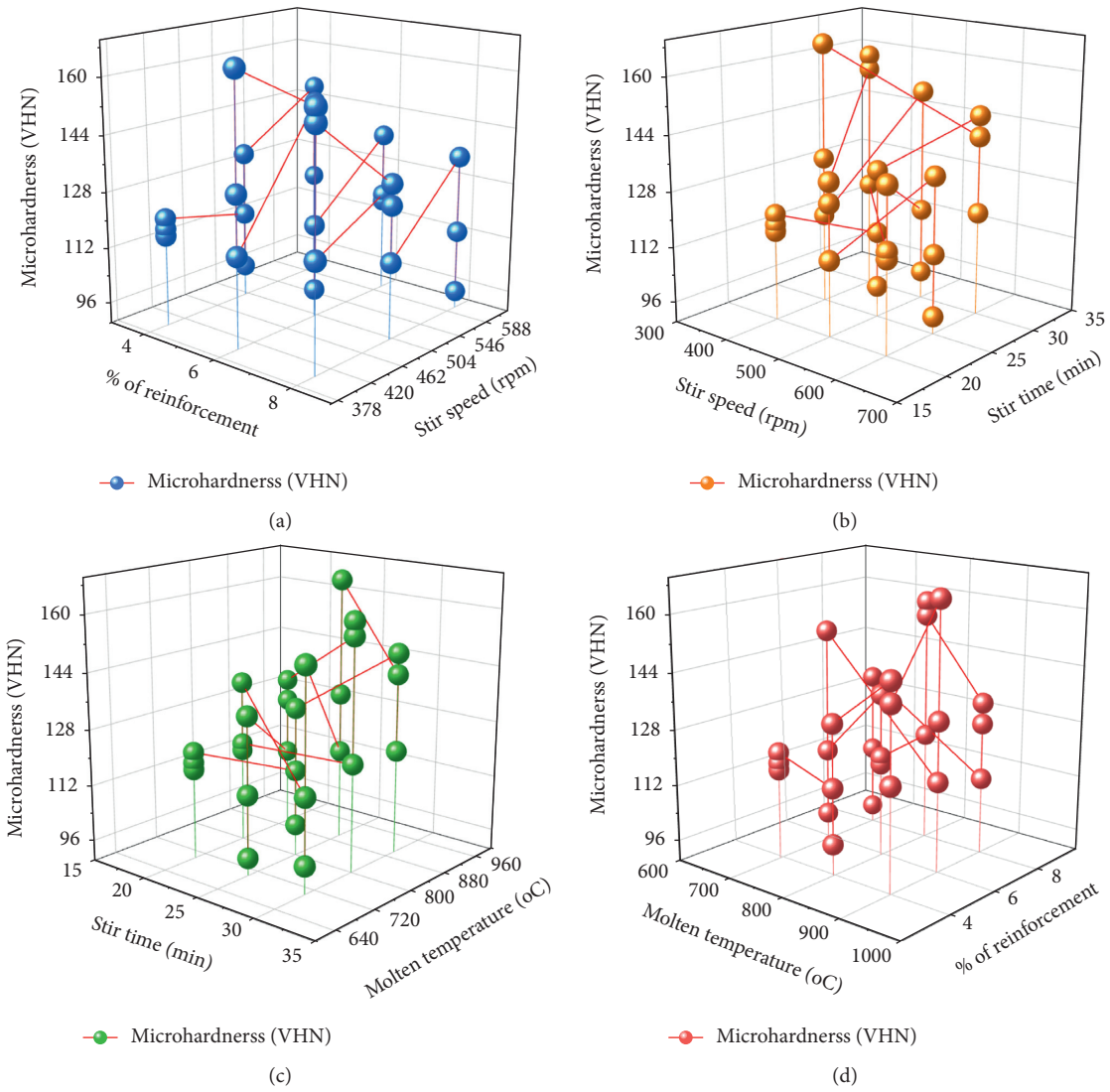

Figure 8: 3D Trajectory plot for microhardness: (a) % of reinforcement vs stir speed; (b) stir speed vs stir time; (c) stir time vs molten temperature; (d) molten temperature vs % of reinforcement.

provides the maximum hardness by the influence of 25 min of stir time and 900 °C of molten temperature. Figure 8(d) represents the maximum microhardness by the influence of 900 °C of molten temperature and 8% of reinforcement. Maximum microhardness was recorded at 8% of reinforcement and 400 rpm of stir speed. The microhardness tends to increase in a linear mode when the % of reinforcement is increased from 4% to 8%. Microhardness tends to decrease when the stir speed is increased from 400 rpm to 600 rpm. The maximum microhardness is encountered at maximum reinforcement % and minimum stir speed. Maximum microhardness was recorded at 400 rpm of stir speed and at 30 min of stir time. The microhardness tends to increase in a linear mode when the stir time is increased from 20 min to 30 min. The microhardness tends to decrease when the stir speed is increased from 400 rpm to 600 rpm. The maximum microhardness is encountered at maximum stir time and minimum stir speed. Higher microhardness

was recorded at 900 ^{0}C of molten temperature and at 30 min of stir time. The microhardness tends to increase in a linear mode when the molten temperature and stir time are increased gradually. The maximum microhardness is encountered at maximum stir *t*. The microhardness was recorded with the highest value when the molten temperature was 900 ^{0}C and at 8% of reinforcement. The microhardness tends to increase in a linear mode when the molten temperature and % of reinforcement are increased gradually. The maximum microhardness is encountered at the maximum % of reinforcement and maximum molten temperature.

5. Conclusion

Hybrid composites such as aluminium alloy (AA8014) with the reinforcement of silicon nitride and zirconium oxide were prepared by a stir casting process successfully. The stir casting parameters were optimized, and the minimum wear values and maximum microhardness values were evaluated in a great manner. Taguchi's optimization method has been used to analyze the results and obtain the optimized parameters based on the S/N ratio. Results of this investigation were demonstrated as follows:

(i) In wear analysis, the minimum wear was recorded as 0.095 mm^3/m by the influence of 4% of reinforcement, 600 rpm of stir speed, 30 min of stir time, and 900 ^{o} C of molten temperature. In the wear test, the percentage of reinforcement was exceedingly influenced. Optimum parameters were registered in the wear test as 8% of reinforcement, 400 rpm of stir speed, 30 min of stir time, and 900 ^{0}C of molten temperature. From the wear analysis, the percentage of reinforcement was extremely influenced such as it was contributed as 7.06%, followed by the stir time (5.05%), stir speed (2.47%), and molten temperature (1.29%).

(ii) Similarly, in microhardness analysis, the maximum hardness was found as 166 VHN by 6% of reinforcement, 400 rpm of stir speed, 25 min of stir time, and 900 ^{o} C of molten temperature. From the microhardness analysis, the molten temperature parameter was exceptionally influenced. Optimum parameters were recorded in the microhardness analysis as 8% of reinforcement, 400 rpm of stir speed, 30 min of stir time, and 900 ^{0}C of molten temperature. In the microhardness analysis, a higher contribution was registered by the molten temperature such as 11.15%, followed by the stir time (7.79%), stir speed (4.07%), and percentage of reinforcement (1.10%).

(iii) Upon validation, the wear was found to be 0.1512 mm^3/min. This was found to be 69.16% much lesser than the average of the wear obtained during the experimentation. Also, the wear of the validated experiment is 18.98% higher than the predicted value. Similarly, the microhardness of the optimal controlling parameters was 142.21 VHN. The microhardness under optimal conditions is 10.90% higher than the average microhardness obtained through the experimentation. Also, the microhardness of the validated experiment is 3% lower than the predicted value. [31, 32].

Data Availability

The data used to support the findings of this study are included in the article.

Conflicts of Interest

The authors declare that there are no conflicts of interest regarding the publication of this paper.

Acknowledgments

The authors thank the Management of Saveetha school of Engineering, SIMATS, Saveetha University, for their appreciation and encouragement to complete this research work with in-house research facilities. It was performed as a part of the Employment Hawassa University, Hawassa, Ethiopia.

References

[1] C. Jia, P. Zhang, W. Xu, and W. Wang, "Neutron shielding and mechanical properties of short carbon fiber reinforced aluminium 6061-boron carbide hybrid composite," *Ceramics International*, vol. 47, no. 7, pp. 10193–10196, 2021.

[2] J. Zhu, W. Jiang, G. Li, F. Guan, Y. Yu, and Z. Fan, "Microstructure and mechanical properties of SiCnp/Al6082 aluminum matrix composites prepared by squeeze casting combined with stir casting," *Journal of Materials Processing Technology*, vol. 283, Article ID 116699, 2020.

[3] C. Saravanan, S. Dinesh, and V. Vijayan, "Assessment on effect of silicon carbide and copper reinforcement on AL7075 alloy," *AIP Conference Proceedings*, vol. 2378, 2021 https://doi.org/10.1063/5.0058505, Article ID 020025.

[4] M. Irfan Ul Haq, A. Raina, A. Anand, S. M. Sharma, and R. Kumar, "Elucidating the effect of MoS2 on the mechanical and tribological behavior of AA7075/Si3N4 composite," *Journal of Materials Engineering and Performance*, vol. 29, no. 11, pp. 7445–7455, 2020, https://doi.org/10.1007/s11665-020-05197-8.

[5] D. K. Q. Mu, Z. Zhang, Y. H. Xie, and J. M. Liang, "The microstructures and mechanical properties of a 5vol%SiC/AA2024 nanocomposite fabricated by powder metallurgy," *Materials Characterization*, vol. 175, 2021 https://doi.org/10.1016/j.matchar.2021.111090.

[6] D. Dey, A. Bhowmik, and A. Biswas, "Effect of SiC content on mechanical and tribological properties of Al2024-SiC composites," *Silicon*, 2020, https://doi.org/10.1007/s12633-020-00757-y.

[7] A. Bhowmik, D. Dey, and A. Biswas, "Tribological behaviour of aluminium-titanium diboride (Al7075-TiB2) metal matrix composites prepared by stir casting process," in *Materials Today Proceedings*, pp. 2000–2004, Elsevier, Amsterdam, 2019.

[8] M. I. Ul Haq and A. Anand, "Dry sliding friction and wear behavior of AA7075-Si3N4 composite," *Silicon*, vol. 10, no. 5,

pp. 1819–1829, 2018, https://doi.org/10.1007/s12633-017-9675-1.

[9] G. Manohar, K. M. Pandey, and S. R. Maity, "Effect of sintering mechanisms on mechanical properties of AA7075/B4C composite fabricated by powder metallurgy techniques," *Ceramics International*, vol. 47, no. 11, pp. 15147–15154, 2021.

[10] N. Ramadoss, K. Pazhanivel, and G. Anbuchezhiyan, "Synthesis of B4C and BN reinforced Al7075 hybrid composites using stir casting method," *Journal of Materials Research and Technology*, vol. 9, no. 3, pp. 6297–6304, 2020, https://doi.org/10.1016/j.jmrt.2020.03.043.

[11] L. Zhang, G. Shi, K. Xu et al., "Phase transformation and mechanical properties of B4C/Al composites," *Journal of Materials Research and Technology*, vol. 9, no. 2, pp. 2116–2126, 2020, https://doi.org/10.1016/j.jmrt.2019.12.042.

[12] M. Rouhi, M. Moazami-Goudarzi, and M. Ardestani, "Comparison of effect of SiC and MoS2 on wear behavior of Al matrix composites," *Transactions of Nonferrous Metals Society of China*, vol. 29, no. 6, pp. 1169–1183, 2019.

[13] S. Jayaprakash, S. Siva Chandran, T. Sathish et al., "Effect of tool profile influence in dissimilar friction stir welding of aluminium alloys (AA5083 and AA7068)," *Advances in Materials Science and Engineering*, vol. 2021, Article ID 7387296, 2021.

[14] S. Arunkumar and A. S. Kumar, "Studies on egg shell and SiC reinforced hybrid metal matrix composite for tribological applications," *Silicon*, vol. 13, 2021, https://doi.org/10.1007/s12633-021-00965-0.

[15] N. S. Sachinkumar, S. Narendranath, and D. Chakradhar, "Microstructure, hardness and tensile properties of friction stir welded aluminum matrix composite reinforced with SiC and fly ash," *Silicon*, vol. 11, no. 6, pp. 2557–2565, 2019, https://doi.org/10.1007/s12633-018-0044-5.

[16] Y. Pazhouhanfar and B. Eghbali, "Microstructural characterization and mechanical properties of TiB2 reinforced Al6061 matrix composites produced using stir casting process," *Materials Science and Engineering: A*, vol. 710, pp. 172–180, 2018, https://doi.org/10.1016/j.msea.2017.10.087.

[17] S. Mosleh-Shirazi and F. Akhlaghi, "Tribological behavior of Al/SiC and Al/SiC/2 vol%Gr nanocomposites containing different amounts of nano SiC particles," *Materials Research Express*, vol. 6, Article ID 065039, 2019.

[18] B. Vinod, S. Ramanathan, V. Ananthi, and N. Selvakumar, "Fabrication and characterization of organic and in-organic reinforced A356 aluminium matrix hybrid composite by improved double-stir casting," *Silicon*, vol. 11, no. 2, pp. 817–829, 2019.

[19] A. Radha, S. Suresh, G. Ramanan, V. Mohanavel, and C. Emmy Prema, "Processing and characterization of mechanical and wear behavior of Al7075 reinforced with B4C and nano graphene hybrid composite," *Materials Research Express*, vol. 6, no. 12, Article ID 1265c5, 2020.

[20] T. Sathish, N. Sabarirajan, and R. Saravanan, "Nano-alumina reinforcement on AA 8079 acquired from waste aluminium food containers for altering microhardness and wear resistance," *Journal of Materials Research and Technology*, vol. 14, pp. 1494–1503, 2021, https://doi.org/10.1016/j.jmrt.2021.07.041.

[21] P. R. Jadhav, B. R. Sridhar, M. Nagaral, and J. I. Harti, "Mechanical behavior and fractography of graphite and boron carbide particulates reinforced A356 alloy hybrid metal matrix composites," *Advanced Composites and Hybrid Materials*, vol. 3, no. 1, pp. 114–119, 2020.

[22] T. Tamizharasan, N. Senthilkumar, V. Selvakumar, and S. Dinesh, "Taguchi's methodology of optimizing turning parameters over chip thickness ratio in machining P/M AMMC," *SN Applied Sciences*, vol. 1, no. 2, p. 160, 2019, https://doi.org/10.1007/s42452-019-0170-8.

[23] N. Ahamad, A. Mohammad, K. K. Sadasivuni, and P. Gupta, "Structural and mechanical characterization of stir cast Al-Al2O3-TiO2 hybrid metal matrix composites," *Journal of Composite Materials*, vol. 54, no. 21, pp. 2985–2997, 2020.

[24] N. K. Bhoi, H. Singh, and S. Pratap, "Developments in the aluminum metal matrix composites reinforced by micro/nano particles - a review," *Journal of Composite Materials*, vol. 54, no. 6, pp. 813–833, 2020.

[25] T. Ye, Y. Xu, and J. Ren, "Effects of SiC particle size on mechanical properties of SiC particle reinforced aluminum metal matrix composite," *Materials Science and Engineering: A*, vol. 753, pp. 146–155, 2019.

[26] C. Fenghong, C. Chang, W. Zhenyu, T. Muthuramalingam, and G. Anbuchezhiyan, "Effects of silicon carbide and tungsten carbide in aluminium metal matrix composites," *Silicon*, vol. 11, no. 6, pp. 2625–2632, 2019.

[27] S. A. A. Daniel, M. Sakthivel, P. M. Gopal, and S. Sudhagar, "Study on tribological behaviour of Al/SiC/MoS2 hybrid metal matrix composites in high temperature environmental condition," *Silicon*, vol. 10, no. 5, pp. 2129–2139, 2018.

[28] J. J. M. Hillary, R. Ramamoorthi, J. D. J. Joseph, and C. S. J. Samuel, "A study on microstructural effect and mechanical behaviour of Al6061–5% SiC–TiB2 particulates reinforced hybrid metal matrix composites," *Journal of Composite Materials*, vol. 54, no. 17, pp. 2327–2337, 2020.

[29] M. B. A. Shuvho, M. A. Chowdhury, M. Kchaou, B. K. Roy, A. Rahman, and M. A. Islam, "Surface characterization and mechanical behavior of aluminum based metal matrix composite reinforced with nano Al2O3, SiC, TiO2 particles," *Chemical Data Collections*, vol. 28, Article ID 100442, 2020.

[30] A. D. Chandio, M. B. Ansari, S. Hussain, and M. A. Siddiqui, "Silicon carbide effect as reinforcement on aluminium metal matrix composite," *J. chem. soc. pak*, vol. 41, no. 4, pp. 650–654, 2019.

[31] R. Venkatesh, D. Sethi, V. Kolli, and B. Saha Roy, "Experimental investigation of aluminium matrix composite production and joining," *Materials Today Proceedings*, vol. 18, pp. 5276–5285, 2019.

[32] G. Jegan, P. Kavipriya, T. Sathish, S. DineshKumar, T. SamrajLawrence, and T. Vino, "Synthesis, mechanical, and tribological performance analysis of stir-casted AA7079: ZrO2 + Si3N4 hybrid composites by Taguchi route," *Advances in Materials Science and Engineering*, vol. 2021, Article ID 7722370, 15 pages, 2021.